Available online at www.sciencedirect.com
SCIENCE DIRECT®
Biochemical and Biophysical Research Communications 327 (2005) 84–93
BBRC
www.elsevier.com/locate/ybbrc

Alternative promotion of the mouse acyl-CoA synthetase 6 (mAcsl6) gene mediates the expression of multiple transcripts with 5′-end heterogeneity: genetic organization of mAcsl6 variants

Eun Ju Lee[a], Hi Chul Kim[b], Yong Yeon Cho[c,1], Sung June Byun[d], Jeong Mook Lim[a], Zae Young Ryoo[c,*]

[a] *Embryology and Gamete Biotechnology, School of Agricultural Biotechnology, Seoul National University, San 56-1, Shilim-Dong, Kwanak-Gu, Seoul 151-742, Republic of Korea*
[b] *Department of Animal Science Graduate School of Konkuk University, Hwayang-dong, Gwangjin-gu, Seoul 143-701, Republic of Korea*
[c] *School of Life Science and Biotechnology, Kyungpook National University, Daegu 702-701, Republic of Korea*
[d] *National Livestock Research Institute, RDA, 564 Oh Mock-Dong, Suwon, Kyonggi-Do, 441-706, Republic of Korea*

Received 23 November 2004
Available online 8 December 2004

Abstract

We report four variants and alternative promoter usage for the mouse acyl-CoA synthetase 6 (mAcsl6) gene. The variants, which were organized into 26 exons and 25 introns spanning 55 kb of DNA on mouse chromosome 11, were classified according to their 5′-UTRs and alternative splicing of exon 13. Alignment of the nucleotide sequences showed that the mAcsl6 variant 1 (mAcsl6_v1) and mAcsl6_v2 used a different promoter and had different splicing patterns than mAcsl6_v3 and mAcsl6_v4. The results of the promoter analysis suggest that the mAcsl6 promoter 1 (mAcsl6_pr1) region has a negative regulatory function. To verify this result, we constructed *id* vector constructs that contained the promoter regions mAcsl6_pr1 and 2, and the chimeric transcript. Although the mAcsl6_pr1 region was deleted, the mAcsl6_v1 and 2 transcripts were detected consistently.

Keywords: mAcsl6 variants; Organization; Alternative splicing; Alternative promoter; *id* vector

Long-chain acyl-CoA synthetase (ACSL, EC 6.2.1.3) catalyzes the initial step in mammalian long-chain fatty acid metabolism. In this reaction, ACSL ligates fatty acids to CoA in a two-step reaction [1,2]: (1) fatty acid + ATP → fatty acyl-AMP + pyrophosphate; and (2) fatty acyl-AMP + CoA → fatty acyl-CoA + AMP [3]. Long-chain acyl-CoAs play a central role in cellular metabolism, being involving in lipid biosynthesis, energy production by β-oxidation, cellular signal transduction [4,5], vesicular trafficking [6,7], modulation of neutrophil function [8], and activation of ryanodine-like receptor, which is involved in Ca^{2+} release in pancreatic acinar cells [9]. In addition, long-chain acyl-CoAs have been implicated as ligands for the transcriptional factors HNF-4α [10] and FadR [11]. Given the multiple roles of long-chain acyl-CoAs, it is clear that ACSL occupies a pivotal role in cellular homeostasis [12]. To date, the five different ACSLs that have been identified show various tissue distributions. ACS1 and ACS5 are expressed prominently in the liver and adipocytes, ACS4 is expressed in steroidogenic tissues, including the adrenal gland, ovary, and testis, and ACS5 is expressed in the intestine [13–16]. ACS2 and ACS3 are expressed predominantly in brain and neural cell lines, although their developmental expression patterns differ [17,18]. These

* Corresponding author. Fax: +82 2 590 2441.
E-mail address: jaewoong64@hanmail.net (Z.Y. Ryoo).
[1] Present address: The Hormel Institute, University of Minnesota, Austin, MN, USA.

0006-291X/$ - see front matter © 2004 Elsevier Inc. All rights reserved.
doi:10.1016/j.bbrc.2004.11.141

findings suggest that each ACSL plays a distinct role in different tissue or at different developmental stages.

Recently, Coleman and co-workers [3] revised the nomenclature system for ACS family members, which has led to some confusion in the scientific literature. They re-classified the ACSLs along the lines of the original human ACSL nomenclature. According to this system, the previously named rodent ACS2 is not orthologous to human fatty acid-CoA ligase 2 (FACL2) [19], and is therefore re-designated as rat Acsl6 (rAcsl6), as it shares highest sequence identity with the human ACSL6, which was originally characterized as LACS5 [20].

The human ACSL6 (originally termed LACS5) was identified in an erythroleukemic cell line and found to be distinct from other cloned members of the human ACSL family. This enzyme uses long-chain fatty acids as substrate, and the mRNA for this protein is highly expressed in erythrocyte precursors and the human brain, whereas it is largely absent from other tissues, including the lung, liver, kidney, heart, and muscle [20]. In the case of the rat, the Acsl6 gene was cloned from brain cDNA libraries in 1992 [17]. Recently, it has been reported that during neurite outgrowth in PC12, rAcsl6 enhances fatty acid internalization and increases the ability to activate fatty acids, which may be incorporated subsequently into phospholipid synthesis, thereby generating extensive neuritis [21]. Therefore, more specific characterization of ACSL6 is needed, since ACSL6 is expressed specifically in the brain and is associated with neuronal development and disease.

In this study, we characterized a mouse homolog of the hACSL6 gene and found this gene to be highly conserved among different species. This suggests that functional analysis of the Acsl6 gene in mice provides useful information on the physiological significance of ACSL6 in other species, including humans. To elucidate the mechanisms that regulate ACSL6 gene expression, we characterized mAcsl6 gene transcription. We found that mAcsl6 has several novel transcripts, which are regulated by an alternative promoter and translated into different isoforms of the mACSL6 protein.

Materials and methods

Cell culture. The mouse neuroblastoma cell line NB41A3 was grown at 37 °C in RPMI 1640 medium (Gibco-BRL, Gaithersburg, MD, USA) that was supplemented with penicillin/streptomycin and 10% fetal bovine serum (HyClone, Logan, UT, USA) in a 5% CO_2atmosphere. The rat glioma cell line C6 was cultured in DMEM (Gibco-BRL). The cells were maintained at 90% confluence and the medium was changed every 3 days.

5′-RACE. Reverse transcription (RT)-polymerase chain reaction (PCR) amplification of the 5′-end of the mAcsl6 cDNA (5′-RACE) was performed using the SMART RACE cDNA Amplification kit (BD Biosciences Clontech, Palo Alto, CA, USA) according to the manufacturer's recommended protocol. For the first-strand cDNA synthesis, 5 μg of total RNA from the adult C57BL/6 mouse brain was combined with the 5′-RACE CDS primer (5′-$(T)_{25}N_{-1}$N-3′), SMART II A oligonucleotide (5′-AAGCAGTGGTATCAACGAAGAGTA CGCGGG-3′), and Superscript II RNase H reverse polymerase (Invitrogen, Carlsbad, CA, USA) in a 10-μl reaction volume. The 5′-end DNA fragments were amplified using 1 μl cDNA, adaptor primer, and common antisense primer for the mAcsl6 gene (5′-GGGT CTGCATCTTCTCCAGAAGTGAGAGAG-3′) or specific antisense primers for the mAcsl6 variants (Vr-1R: 5′-TTCCTTTACT GTGTGC CTGGCATCTACTCC-3′; 2R: 5′-GCCTGTGGGAACA GGTCTTG TAGGGACCAA-3′; 3R: 5′-GGAGTAGATGCCAGGC ACACAG TAAAGGAA-3′; and 4R: 5′-GGTTTTATGGCTAGG CAGGCTC AAATGGCA-3′ (Fig. 1B). PCR was conducted with 3-min denaturation at 94 °C, followed by 35 cycles of 94 °C for 15 s, 55 °C for 30 s, 68 °C for 3 min, and a 7-min final extension step at 68 °C. The DNA fragments were introduced directly into the pCR 2.1-TOPO (Invitrogen) vector and sequenced.

RT-PCR. RNA was isolated from various tissues of the C57BL/6 mouse. Total RNA (5 μg) was treated with RNase-free DNase I (Takara, Tokyo, Japan) and then reverse-transcribed with AMV reverse transcriptase using oligo(dT) (N15). The cDNAs of various tissues were used for PCR, which consisted of a 5-min denaturation step at 95 °C, followed by 40 cycles of 1 min at 94 °C, 1 min at 65 °C, 2 min at 72 °C (25 PCR cycles for the β-actin internal control), and a final elongation step of 10 min at 72 °C. The primer sequences used were identical to those described for the detection of the full-length cDNAs.

Isolation of full-length mAcsl6 cDNA. The following variant-specific primers were designed using the sequences of the 5′-RACE cDNA fragments: Vr-1F, 5′-GCATGTGCACTTTCTGGGACAG-3′; Vr-2F, 5′-GACATGCTGACCTTCTTCTTGG-3′; Vr-3F, 5′-GCTGGTTCT AGCAGAATCAGCT-3′; Vr-4F, 5′-TCTTATTTGAGAAGAGGT CCA-3′; and A2R ter, 5′-CACACGGAGACTAAGTAAAGC-3′ (Fig. 1B). Aliquots (5 μg) of total RNA from the adult C57BL/6 mouse brain were reverse-transcribed, amplified, and introduced into the pCR2.1-TOPO vector. The cDNAs were confirmed by restriction mapping and DNA sequencing analyses, and examined for homology with the mouse genome sequence (http://www.ncbi.nlm.nih.gov/genome/seq/MmBlast.html).

Real-time PCR analysis. The cDNAs from brains at each developmental stage were used for real-time PCR, using SYBR Green I dye chemistry with the following variant-specific primers: for mAcsl6_v1, RV-1F 5′-ACTTCAGCATGTGCACTTTCT-3′ and RA2-1 5′-CCGCAGGATCCTCAGGAT-3′; for mAcsl6_v2, RV-2F 5′-GACA TGCTGACCTTCTTCTT-3′ and RA2-1; for mAcsl6_v3, RV-3F 5′-GAGAAGATTCAGAGGAACAT-3′ and RA2-2 5′-AAGTGAGAG AGCAATCT**CTTT**-3′; and for mAcsl6_v4, RV-4F 5′-AGATG TGGTAACCTCTTTCC-3′ and RA2-1.

To detect bands specific for the mAcsl6_v3 variant, the RA2-2 primer was distinguished by four bases (bold letters) in exon 3a. Real-time PCR product accumulation was monitored using the Rotor-Gene 2000 (Corbett Research, Sydney, Australia). The amplification program included an initial denaturation step at 95 °C for 5 min, followed by 37 cycles of denaturation at 94 °C for 15 s, annealing at 60 °C for 20 s, and extension at 72 °C for 15 s. SYBR Green fluorescence was measured after each extension step. The specificity of amplification was assayed by melting curve analysis. The mean cycle threshold value (C_t) from triplicate samples was used to calculate the gene expression level. The levels of PCR products were normalized to the levels of β-actin product. The following β-actin-specific primers were used: forward, 5′-TCACCCACACTGTGCCCATCTACGA-3′ and reverse, 5′-CGAAGTCTAGAGCAACATAGCAC-3′.

Production of mAcsl6 antibody. The mAcsl6_v1 full-length cDNA was introduced into the *Eco*RI/*Hin*dIII site of the pET-28b (Novagen, Darmstadt, Germany) bacterial expression vector, to generate pET28b-mAcsl6, which was transformed into *Escherichia coli* strain BL21. The bacterial cultures were grown to $OD_{600} = 0.6$ and then induced with isopropyl-β-D-thiogalactopyranoside (IPTG), followed

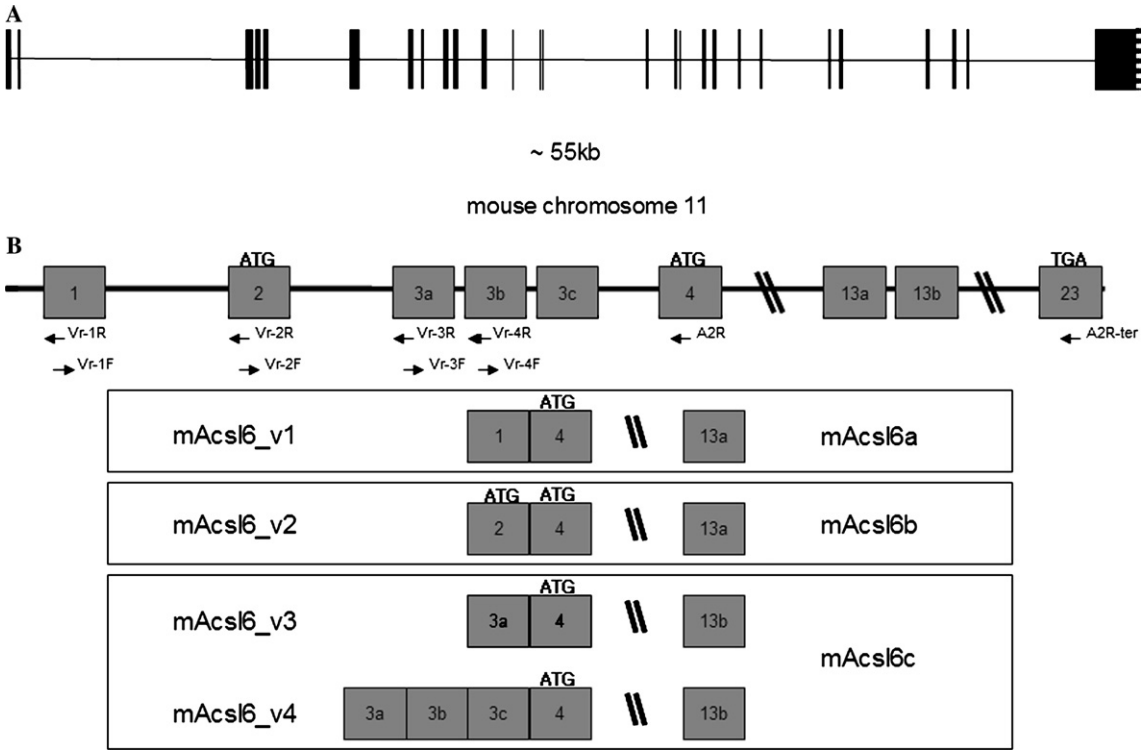

Fig. 1. (A) Genomic structure of the mAcsl6 gene. The exons are represented by closed boxes and the introns are indicated by horizontal lines. The schematic representation was derived by assembling the two genomic sequences with GenBank Accession Nos. AL596127 and AL603822 into a contig of 55 kb, which contains the cDNAs of the mAcsl6 variants. (B) Scheme for the mAcsl6 cDNA variants mAcsl6_v1, 2, 3, and 4, and the protein isoforms mAcsl6a, b, and c. The exons are represented by numbered boxes. The second transcription variant mAcsl6_v2 differs from the other variants in having an in-frame ATG in exon 2. For this reason, the mAcsl6 protein isoform 2 mAcsl6b is 81 kDa, i.e., about 3 kDa larger than the other variants. The mAcsl6_v3 and 4 variants have replaced exon 13a with 13b, which results in a 12 amino acid substitution without a size change. The sequences of the PCR primers that were used to identify the transcription start sites and amplify the full-length cDNAs of the transcription variants are indicated by arrows.

by culturing for an additional 3 h at 37 °C. The bacteria were pelleted by centrifugation, resuspended in lysis buffer [150 mM NaCl, 10 mM Tris (pH 7.2), 0.1% SDS, 1.0% deoxycholate, and 5 mM EDTA], and disrupted with a series of 15 2-s bursts of sonication. The lysate was centrifuged, the pellet was resuspended in 6 M urea solution [6 M urea, 20 mM Tris (pH 8.0), and 500 mM NaCl], and the mAcsl6 protein was purified on a His-binding resin (Novagen) according to the manufacturer's recommended protocols. The purity of the eluted protein was confirmed by SDS–PAGE and Western blotting with His tag antibody (Santa Cruz Biotechnology, Santa Cruz, CA, USA). The purified protein was used as an antigen for the production of anti-mAcsl6 antibodies in rabbits. The immunoglobulin G (IgG) fraction was purified using the HiTrap Protein G column (Amersham–Pharmacia Biotech, Buckinghamshire, UK) and designated as the anti-mAcsl6 antibody.

Western blot analysis. Tissues from the adult C57BL/6 mouse were homogenized and centrifuged at 3000 rpm for 10 min, and the supernatant fluid was recovered. To isolate the membrane fraction, the supernatants were centrifuged at 41,000 rpm for 40 min, and the pellets were resuspended in membrane fraction suspension buffer [50 mM Tris (pH 8.0), 150 mM NaCl] using a Teflon-glass homogenizer. All of the procedures were carried out at 4 °C. The membrane fraction proteins were separated by SDS–PAGE, transferred onto a nitrocellulose transfer membrane (Schleicher & Schuell, Dassel, Germany) and hybridized with the rabbit anti-mAcsl6 antibody (1:500 dilution). The mAcsl6 proteins were visualized with horseradish peroxidase (HRP)-conjugated anti-rabbit IgG sheep secondary antibody (1:2000 dilution) and enhanced using chemiluminescence detection reagents (ECL; Amersham–Pharmacia Biotech). For detection of the specific bands reacting with the anti-mAcsl6 antibody in Western blotting analysis, 10 μl of the anti-mAcsl6 antibody was mixed with 100 μl of immunizing antigene (4 μg/μl) in 390 μl PBS solution and incubated for 2 h at 37 °C, and then incubated overnight at 4 °C. The blots were stripped and the analysis was repeated using the immunizing antigen bound to the anti-mAcsl6 antibody and rabbit anti-actin antibody (1:500 dilution; Santa Cruz Biotechnology), to verify loading of equal amounts of protein.

Construction of plasmids for promoter analysis. Constructs with progressive deletions of the mAcsl6 promoter region were engineered by PCR from the genomic DNA of a C57BL/6 mouse. The PCR fragments were generated using a forward primer with a *Bam*HI restriction site and a reverse primer that contained a *Hin*dIII site. The amplified DNA fragments were subcloned into the pCR2.1-TOPO vector that was digested with *Bam*HI/*Hin*dIII, and subsequently subcloned into *Bgl*II/*Hin*dIII-digested pGL3-Basic vector (Promega, Madison, WI, USA), to generate pGLAcsl6. All of the constructs were confirmed by restriction mapping and DNA sequencing. To amplify the high G/C content region of the mAcsl6 promoter region, we used the Advantage-GC Genomic PCR Kit (BD Biosciences Clontech). The reaction conditions used were according to the manufacturer's recommendations.

Reporter gene assay. NB41A3 and C6 cells (1×10^5) were seeded onto six-well tissue culture plates 1 day before transfection. The cells were transfected with each of the promoter reporter plasmids (pGLAcsl6) using Lipofectamine (Invitrogen) following the manufacturer's recommended protocols. The phRL-TK vector (Promega) was

co-transfected with the promoter reporter plasmid, to normalize for transfection efficiency. After incubation for 48 h, the cells were lysed with passive cell lysis buffer (Promega) and centrifuged at 12,000 rpm for 2 min to remove cell debris. The supernatant was used for both the firefly and *Renilla* luciferase activity assays. Luciferase activity was determined using the TD-20/20 luminometer (Turner BioSystems, Sunnyvale, CA, USA). The pGL3-Basic vector was used as a negative control in each transfection experiment.

Construction and analysis of the id vector. The DNA fragment that encompassed the region from mAcsl6_pr1 to the innate intron (1 kb) and the other genomic PCR fragments that included exon 4 were ligated into *Bgl*II/*Nco*I-digested pGL3-Basic. The PCR fragments were generated using reverse primers that contained a *Sal*I site (5′-GTCGACCTATGCATATCTCAGGAGCC-3′) or an *Nco*I site (5′-CCATGGTCTGCATCTTCTCCAGAAG-3′), together with forward primers that contained a *Bam*HI or *Xho*I (5′-CTCGAGGTCCCACCAACCTCCTAGGTTTC-3′) site. We designated this vector as the *id* vector. After construction of the *id* vector, progressive deletions of mAcsl6_pr1 region were engineered by generating PCR fragments that contained *Bam*HI and *Sal*I sites. The fragments were subcloned into the *Bgl*II/*Nco*I-digested pGL3-Basic, together with another fragment that included exon 4. The mAcsl6_pr1-specific sequences for these primers were taken from the mouse genomic contig database. All of the constructs were sequenced from both ends, to ensure correct orientation and fidelity. The various *id* vectors were transfected transiently into NB41A3 cells, and RT-PCR was performed with specific primers for exons 1 (Vr-1F), 2 (Vr-2F), and for the luciferase primer (5′-ACGAACGTGTACATCGACTG-3′).

BLAST sequence similarity searches. The nucleotide and protein BLAST searching programs at NCBI (http://www.ncbi.nlm.nih.gov/BLAST) were used for sequence homology searches in the public databases. The exon–intron organization of mAcsl6 was determined by a BLAST search of the mouse genomic contig database. Multiple sequence alignments were performed using the CLUSTAL W (http://www.ebi.ac.uk/clustalw) and ESPript 2.2 (http://prodes.toulouse.inra.fr/ESPript/cgi-bin/ESPript.cgi) programs.

Results and discussion

Cloning and transcriptional start site identification of the mouse Acsl6 variants

As an initial approach to elucidate the mechanisms that regulate ASCL6 gene expression, we characterized the transcriptional units of the mAcsl6 gene. In humans, it has been reported that ACSL6 variants differ in their amino acid constitutions as a result of alternative exon use (unpublished observations) [3]. The mouse Acsl6 (mAcsl6) cDNA (GenBank Accession No. BC016114) has 93% homology with the rat Acsl6 cDNA (D10041), which shares highest sequence identity with the human ACSL6 [17]. Therefore, the Acsl6 gene appears to be conserved across species. For the isolation of mAcsl6 gene variants, we BLAST searched the databases at NCBI with BC016114 as the query sequence, and screened two positive mouse cDNA clones (NM_144823 and AY167035). The screened clones and query clone had 99% homology in the ORF and 3′-UTR regions but had different 5′-UTRs. To identify the transcription start site, 5′-RACE PCR was performed with the reverse specific primers from a common in-frame ATG of the three clones, together with an adaptor primer. From this result, we obtained two novel mAcsl6 variants that contained different 5′-UTRs. The full-length cDNAs of the mAcsl6 variants were assembled from RT-PCR products that were amplified with the forward-specific primers of the variants identified by 5′-RACE PCR, together with the reverse primer for the common 3′-UTR of mAcsl6. The mAcsl6_v1 variant, which has a 2093-bp ORF that contains exon 13a and a 150-bp 5′-UTR and encodes 697 amino acids (78-kDa protein), was named mAcsl6a. The mAcsl6_v2 variant, which consists of a 2168-bp ORF that contains exon 13a and a 31-bp 5′-UTR and encodes 722 amino acids (81-kDa protein), was named mAcsl6b; the translation start-point was localized 74 nucleotides upstream of the common ATG of the mAcsl6 variants. The mAcsl6_v3 and 4 variants contain a 2093-bp ORF in which exon 13a is replaced with exon 13b, coding for 697 amino acids; the 5′-UTR of mAcsl6_v3 is 297 bp in length, and the 5′-UTR of mAcsl6_v4 is 671 bp in length, and the calculated mass of the mAcsl6c protein is 78 kDa. These transcripts were named in accordance with the established nomenclature system [3]. From the sequence data of mAcsl6_v2, another in-frame ATG triplet was located in the 5′-UTR (Fig. 1B). When mAcsl6_v2 was expressed in BL21, an 81-kDa protein was detected (data not shown).

Using 5′-RACE PCR, we obtained two mAcsl6 variants, mAcsl6_v3 and 4, which had different transcription initiation sites and exon usage than those of the GenBank clones. Thus, we re-estimated the initiation sites of the clones. The mAcsl6_v3 variant was generated by alternative splicing of exon 3b, 3c from mAcsl6_v4 (Fig. 1B). The various mAcsl6 gene variants have been deposited in GenBank (NCBI), with Accession No. AY786360–AY786363.

Genomic DNA organization and mAcsl6 gene alignments

During the cloning of the full-length mAcsl6 cDNA, two genomic clones of the gene were sequenced at the Sanger Centre (Hinxton, UK) and deposited in GenBank, with Accession Nos. AL596127 and AL603822. These two genomic sequences were assembled into a contig of 55 kb, which contained all of the mAcsl6 cDNA sequences. Alignment of this contig with the mAcsl6 variants showed that the mAcsl6 gene comprises 26 exons and 25 introns that span 55 kb of mouse chromosome 11 (Fig. 1A). All the exon/intron boundaries were defined in accordance with the GT/AG rule (Table 1). The results of the organization of the mAcsl6 gene reveal multiple 5′-flanking regions that are spaced 332- to 10,935-bp apart. Alignment of mAcsl6 suggests that the variants were generated from a single mAcsl6 gene, based on the complete match of the nucleotide sequences corresponding to exons 4–23, with the exception of exon

Table 1
Exon–intron boundaries of the mouse Acsl6 gene

Exon	Exon size (bp)	3′ splice acceptor site	5′ splice donor site	Intron size (bp)
1	124		GTGGAG**gt**agggtc	332
2	79		TTGCCG**gt**aagtcc	10,603
3a	271		GGAAAG**gt**aggatg	90
3b	206	cactaa**ag**GACTCT	AGCCTG**gt**gaggca	91
3c	168	tactgc**ag**GTTTCT	AACCAG**gt**gaggcg	4390
4	220	tcctac**ag**AGATTG	GTGGAG**gt**gagcagg	2869
5	114	ttttct**ag**GACGGT	TCTCAG**gt**aaggag	635
6	64	ctctgc**ag**GGAATG	CAAGAG**gt**gagtga	1012
7	101	gtgtgc**ag**GTGGCC	CCGGAG**gt**gaggat	394
8	99	ttctgt**ag**TGGATC	ATACTG**gt**gagccc	1455
9	178	ccctgc**ag**CGGACA	ATAGAG**gt**gagagt	1109
10	32	ttcttc**ag**GACTGT	CCCGTG**gt**aagcta	1486
11	51	ccccgc**ag**CCCCCA	CAACAG**gt**aagccg	5080
12	73	gttttc**ag**GGAACC	ACAGAG**gt**gaataa	1811
13a	78	acctgc**ag**AAAGTG	ATCCAG**gt**aagcct	57
13b	78	tcttgc**ag**AGTCAG	GTGCAG**gt**aaggcc	1264
14	134	tccccc**ag**TCTGTT	GACAAG**gt**gggtcc	454
15	134	ctcctc**ag**ATCTTC	ATTCAG**gt**aaagaa	1363
16	95	tcccac**ag**GCCAGT	TGCCAG**gt**atcatc	1167
17	72	gcttga**ag**GTCTAT	CATCAG**gt**aggaga	3355
18	78	tgtcct**ag**GGCATG	GGAGAG**gt**gaggtt	614
19	116	ccccac**ag**ATATGT	CTGCCG**gt**atgtag	4564
20	143	ctccac**ag**GAGGGA	TTAAAG**gt**gagcac	1321
21	101	ctttgt**ag**GCCTTT	AAAAAG**gt**ctgtac	868
22	71	caattc**ag**GAATTG	GAACAG**gt**aactgac	7998
23	458	gtttttt**ag**GGTTAAA		

The GT/AG rule is shown in bold.

13 (Fig. 2A). The isoforms were classified according to translation start site and exon 13 alternative usage, which resulted in a 12 amino acid substitution without alteration of protein size (Fig. 2B).

Based on the genomic organization results for the mAcsl6 variants, it is possible to classify the deposited GenBank clones NM_144823, AY167035, and BC016114. The NM_144823 clone was not included among the variants that we cloned, and the AY167035 and BC016114 clones had different transcription start sites than the variants (Table 2).

Tissue distribution and developmental expression of mAcsl6 variants

To analyze tissue distribution, we performed RT-PCR with RNA samples from several tissues. All of the mAcsl6 variants were expressed at high levels in the brain and at low levels or not at all in other tissues (Fig. 3A). To monitor the expression patterns of mAcsl6 protein isoforms in various adult mouse tissues, Western blot analysis was performed using the anti-mAcsl6 antibody. Western blotting detected two bands with molecular weights of 78 kDa (mAcsl6a, c) and 81 kDa (mAcsl6b), which were expressed at high levels in the brain only. Although similar bands were detected in the small intestine and stomach, these bands were shown to be artifacts in experiments using the immunizing antigen bound to the anti-mAcsl6 antibody (Fig. 3B).

Using real-time PCR, we characterized the developmental expression patterns of the mAcsl6 variants in the brain. Total RNA samples were extracted from mouse brains on embryonic days 10, 17, and 19, and on postnatal days 0, 5 10, 15, 25, and 30 days, and real-time PCR was performed. Surprisingly, the expression of mAcsl6_v3 increased dramatically from postnatal day (Fig. 3D). The expression levels of the other variants increased slightly during brain development (Figs. 3C and D). These results suggest that mAcsl6_v3 is abundant as mAcs6 protein in the adult brain and may play an important role in brain development.

Functional characterization of the mAcsl6 promoter region

Based on the genomic organization of the mAcsl6 variants, we cloned the three 5′-flanking regions. To assess the promoter activities of the 5′-flanking regions of the mAcsl6 variants, we examined up to 2 kb of the genomic sequences upstream of the determined transcription start sites of mAcsl6_v2 and 1.8 kb of mAcsl6_v3 using computer-based analysis (MatInspector software using Transfac 6.0). Putative binding sites for the transcription factors AP2, C/EBPα, C/EBPβ, CREB, NF-1, and SP1 were identified in the proximal sequences. This analysis suggests that a TATA-less promoter is used for mAcsl6 gene expression.

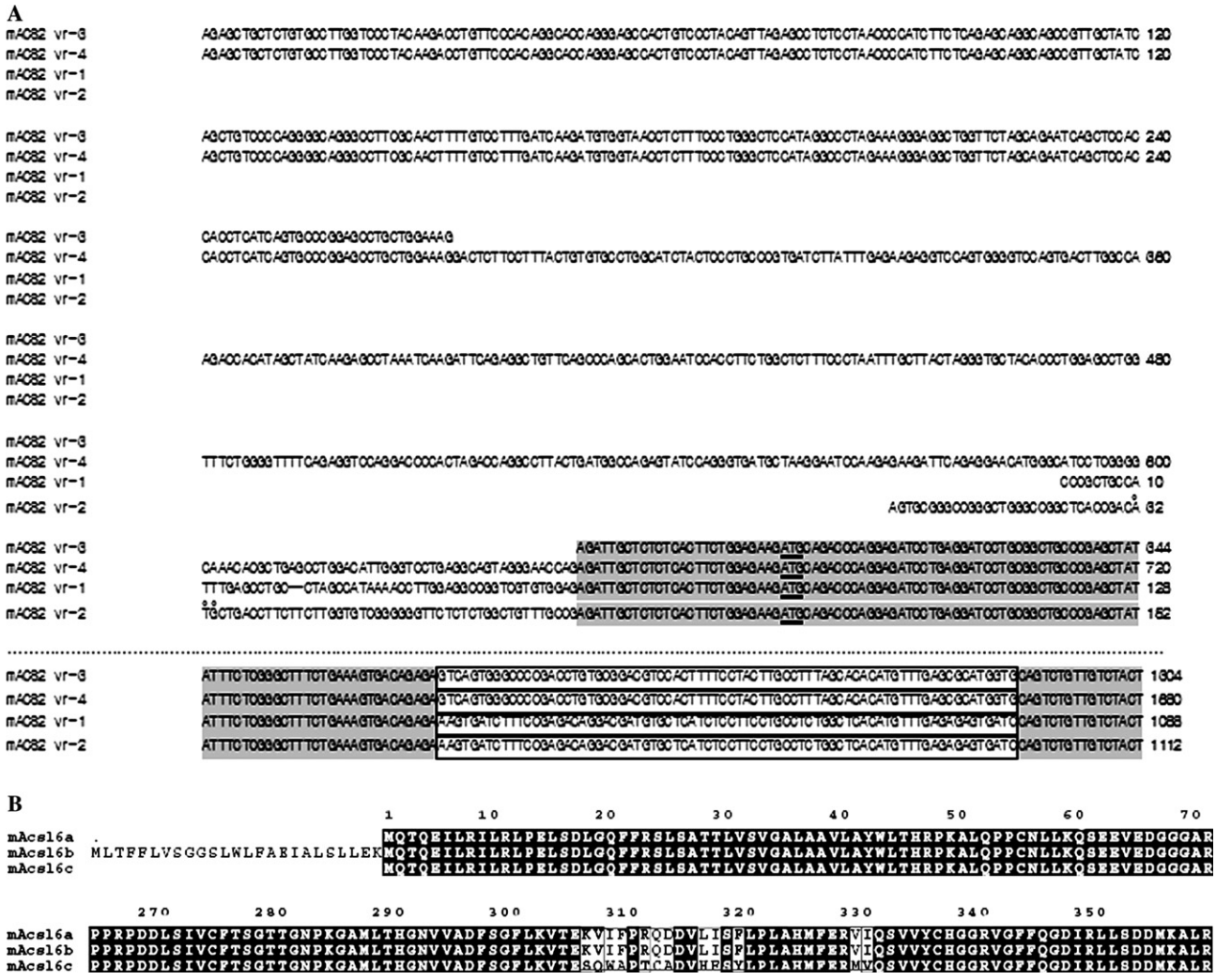

Fig. 2. Alignments of the mAcsl6 variants and protein isoforms. (A) The full-length cDNAs that were isolated from mouse brains were compared using the CLUSTAL W program. (B) The deduced protein isoforms of mAcsl6 were aligned by ESPript 2.2. The common ATG is underlined in black letters, and the corresponding methionine is indicated as 1. In the case of mAcsl6_v2, the ATG upstream of the common ATG is dotted as an initiation codon, and the corresponding methionine in (B) is also dotted. The mAcsl6_v1 and 2 variants contain exon 13a and mAcsl6_3 and 4 are substituted with exon 13b, which results in a 12-amino-acid change without change in protein size, as represented by the white boxes with black letters in (A,B).

Table 2
Classification of previously deposited, novel, and re-evaluated variants according to 5′-untranslated regions and exon 13a or b encoding

Classified according to	Nomenclature	Previous deposited variants
5′-untranslated region	mAcsl6_v1	BC016114/**AY786363**[a]
	mAcsl6_v2	NM_144823/AY167035/**AY786361**
	mAcsl6_v3,4	**AY786362**/**AY786360**
Exon 13a	mAcsl6_v1,2	BC016114/AY167035/**AY786363**/**AY786361**
Exon 13b	mAcsl6_v3,4	NM_144823/**AY786362**/**AY786360**

[a] The GenBank accession numbers of the novel and re-evaluated mAcsl6 variants are shown in bold.

To localize the DNA elements that are important for promoter activity, unidirectional deletion analysis was carried out on up to 2 kb of the 5′-flanking region of the mAcsl6 gene. In the case of mAcsl6_pr1, only background levels of firefly luciferase activity were observed in NB41A3 and C6 cells (Figs. 4A and B). However, when mAcsl6_pr1 and mAcsl6_pr2 were combined, promoter activity was observed and luciferase activity

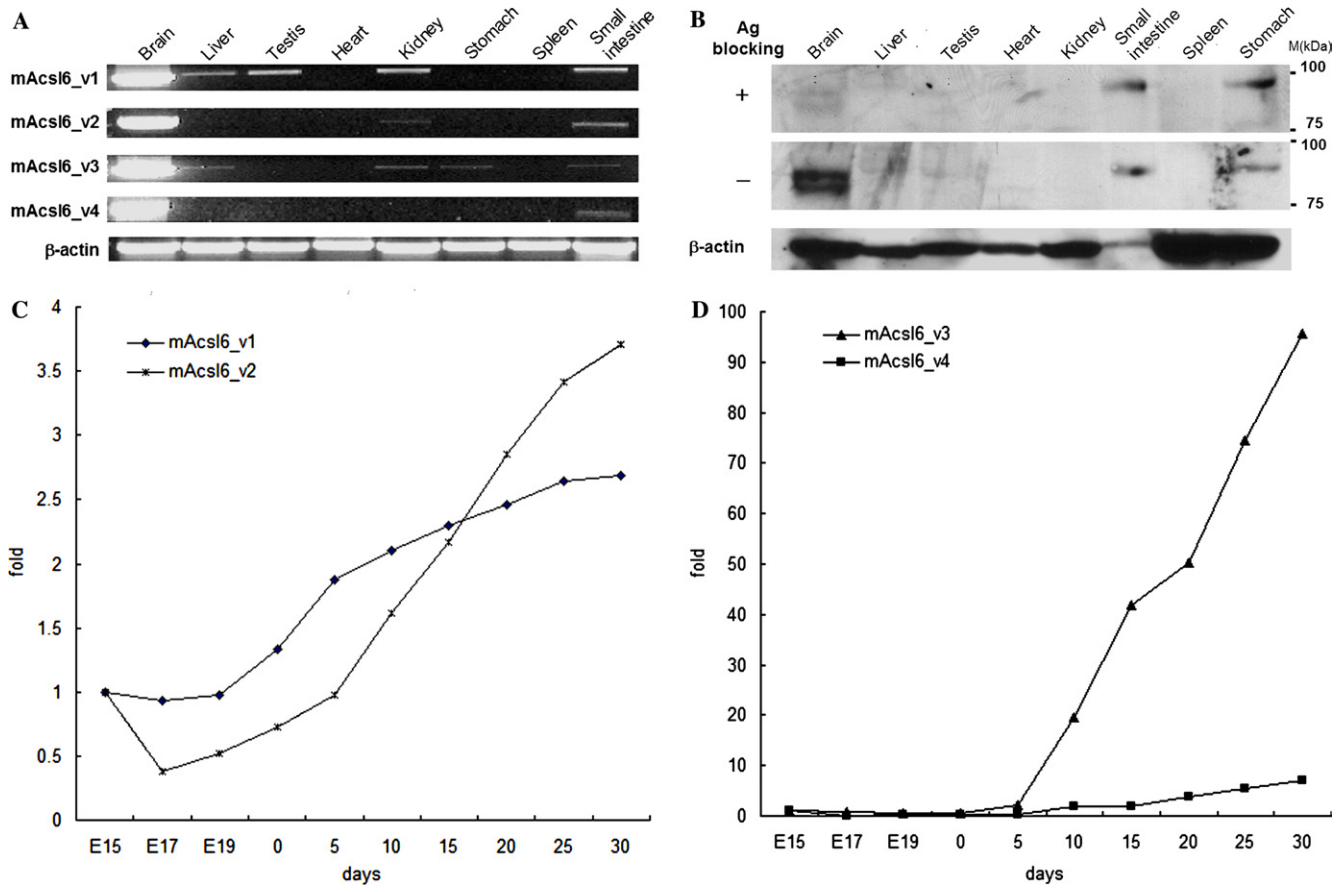

Fig. 3. Tissue distribution of the mAcsl6 gene and differential gene expression of mAcsl6 variants. (A) RT-PCR analysis of the gene expression levels of mAcsl6 variants in various mouse tissues was performed using primers to amplify the full-length cDNAs and using the β-actin gene as the control. The variants were detected mainly in the brain, with minor expression in other tissues following excessive amplification. (B) Western blot analysis was carried out with 100 μg protein from each tissue and the anti-mAcsl6 antibody. The results show two bands: a 78-kDa band that represents mAcsl6a,c, and an 81-kDa band that represents mAcsl6b, both of which are found mainly in the brain tissue. Although similar bands were detected in the small intestine and stomach, these bands were shown to be artifacts in experiments using the immunizing antigen bound to the anti-mAcsl6 antibody. β-Actin was used as the internal control. (C,D) Real-time PCR analysis of mAcsl6 variant expression in different developmental stages of the mouse brain was performed using primers that amplify the specific 5′-UTRs of the variants. The specificity of amplification was subjected to melting curve analysis. The mean cycle threshold value (C_t) from triplicate samples was used to calculate the level of gene expression. The PCR product levels were normalized to the levels of β-actin PCR product. E, embryonic day; 0, birth-point in *X* axis. The results of the real-time PCR show differential expression of mAcsl6 variants in different developmental stages.

was increased more than 13-fold by deletion of the mAcsl6_pr1 region (Fig. 4A). These results indicate that mAcsl6_pr1 inhibits the expression of mAcsl6_v1 and mAcsl6_v2. To determine further the functional importance for promoter activity of the potential transcription factor-binding sites located between −398 and +46, additional progressive deletion constructs were generated. A deletion that extended to nucleotide −31 produced the background level of luciferase activity (Fig. 4A). Thus, the DNA elements located in the region −104 to −31 may contribute to the basal promoter activity of mAcsl6_pr2. In mAcsl6_pr3, luciferase activity did not change when the 5′-flanking sequence length was deleted up to nucleotide −185, which indicates that the motifs located between −1836 and −185 play no significant role in mAcsl6_pr3 activity. A deletion from nucleotides −185 to −9 decreased luciferase activity to the level produced by the pGL3-Basic vector (Fig. 4C). These results suggest that the DNA elements located between −185 and −9 contribute to the basal promoter activity of mAcsl6_pr3.

Regulation of the mAcsl6_v1 and 2 transcripts

In the case of mAcsl6_pr1, promoter activity was similar to that of the pGL3-Basic vector, which suggests that the mAcsl6_pr1 region does not promote the transcription of mAcsl6_v1, but has a negative regulatory function. In support of this hypothesis, we constructed the *id* vector, which contained the mAcsl6_pr1, 2 genomic DNA fragment, the truncated intact intron, and the luciferase gene for the chimeric transcript (Fig. 5A).

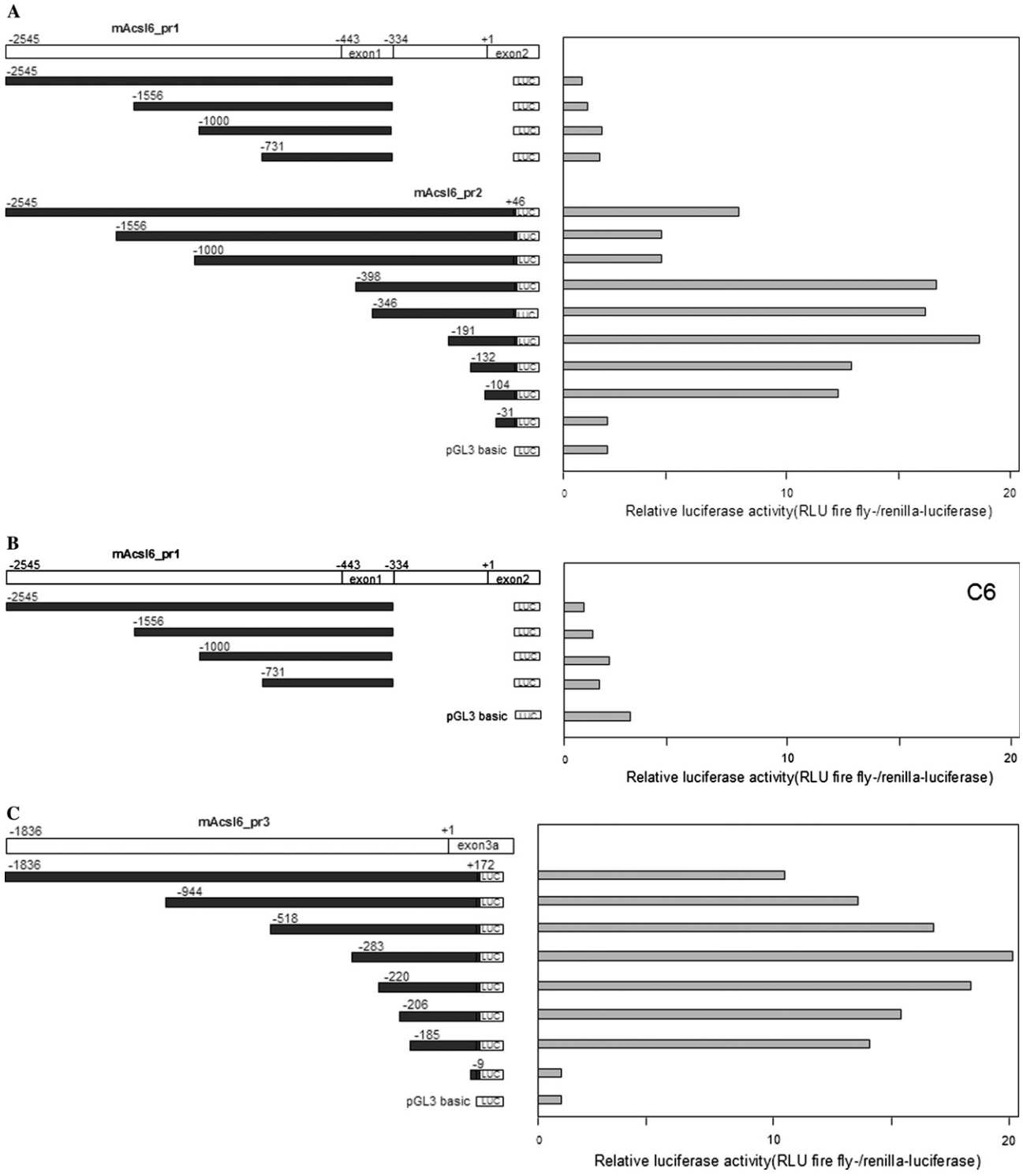

Fig. 4. Structures of the pGLAcsl6 vectors and their activities following transient transfection into NB41A3 or C6 cells. Various fragments from the mAcsl6 promoter region were cloned into the pGL3-Basic vector. The numerical designation of each construct is based on the assignment of the primary transcription start site as +1 for mAcsl6_v2 and v3. The firefly luciferase levels were determined using a luminometer and corrected for transfection efficiency with a *Renilla* luciferase-expressing vector. The values are presented as relative to the activity of the vector pGLAcsl6. The results from three experiments performed in duplicate are shown.

Serial deletion constructs of the mAcsl6_pr1 region in the *id* vector were transfected transiently into NB41A3 cells, and chimeric transcripts were detected by RT-PCR with specific primers for exon 1, 2, and the luciferase primer. The mAcsl6_pr1 variant-containing plasmid *id* (−2545 or −998) showed weak expression of chimeric

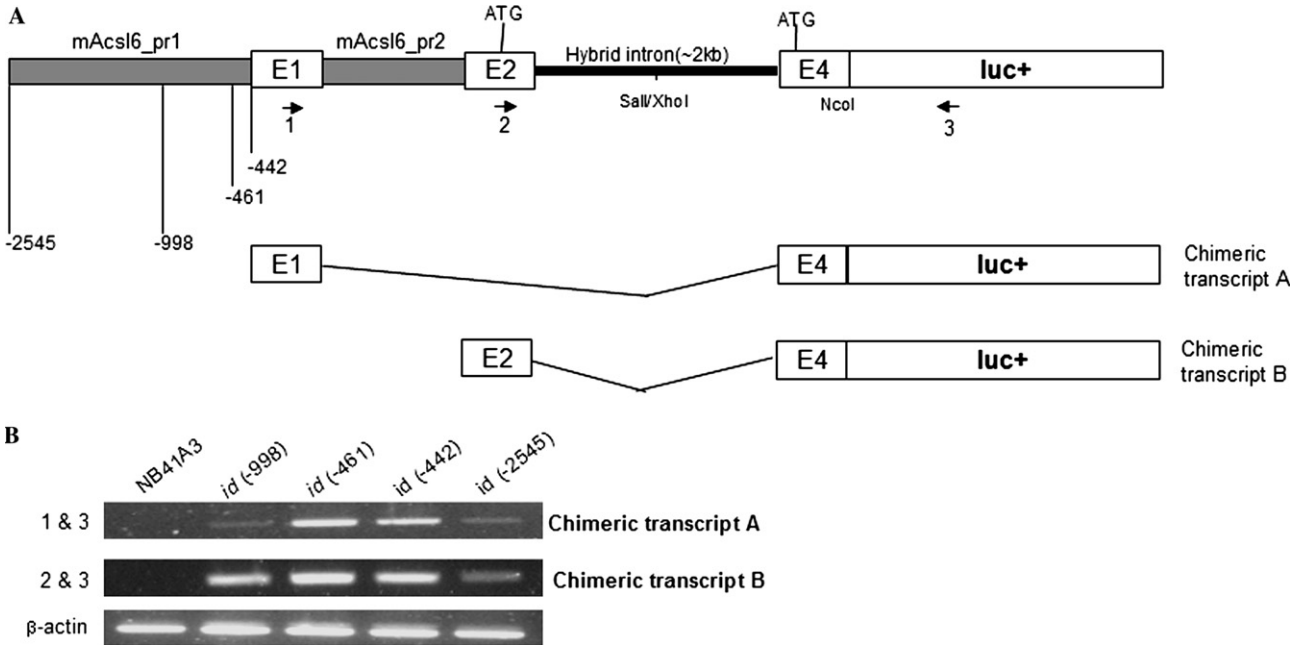

Fig. 5. Functional detection of mAcsl_pr1 through the *id* vector. (A) Structure of the *id* vector, which contains various restriction fragments from the mAcsl6_pr1 region with chimeric transcripts. The numerical designation of each construct is based on the assignment of the primary transcription start site as +1 in mAcsl6_v2, exon 2. (B) RT-PCR of chimeric transcripts. The various *id* vectors were transfected transiently into NB41A3 cells, and RT-PCR was performed with specific primers for exon 1,2 and the luciferase primer. Transcripts were detected faithfully for mAcsl6_v1 and v2 in the *id* vector (−442). The results for one of three representative experiments are shown.

transcripts A and B. Significantly, when mAcsl6_pr1 was deleted to nucleotides −461 or −442, to produce *id* (−461 or −442), the levels of chimeric transcripts A and B were increased (Fig. 5B). These results clearly show that the region of mAcsl6_pr1 between nucleotides −2545 and −461 exerts a negative regulatory function to control mAcsl6_pr2 promoter activity.

The brain is second only to adipose tissue in having the highest concentration of lipids in the body. In the brain, lipids serve primarily to modify the fluidity, structure, and functions of membranes, and homeostasis of lipid metabolism is important for brain development [22,23]. Fatty acids need to be activated to their acyl-CoAs by acyl-CoA synthetases (ACSs) for lipid metabolism, the activities of which have been found in the brain [24,25]. Moreover, Acsl1, Acsl6, and Acsl3 mRNAs have been analyzed in the postnatal rat brain, and only the levels of Acsl6 were found to be elevated during development [18]. Refsum disease is an autosomal recessive neurological disorder that is associated with Acsl6 [26]. During differentiation, neurons require substantial amounts of Acsl6-produced long-chain acyl-CoAs to generate extensive neuritis [21]. These reports suggest pivotal roles for Acsl6 in brain development and neurological disorders in adults.

In summary, we have characterized the mouse homolog of the hACSL6 gene, and demonstrated alternative promoter usage through report assays and the use of the *id* vector.

Acknowledgment

This work was supported by Biogreen 21 (1000520030039000-1).

References

[1] W.W. Cleland, The kinetics of enzyme-catalyzed reactions with two or more substrates or products. I. Nomenclature and rate equations, Biochim. Biophys. Acta 67 (1963) 104–137.
[2] J. Bar-Tana, G. Rose, R. Brandes, B. Shapiro, Palmitoyl-coenzyme A synthetase. Mechanism of reaction, Biochem. J. 131 (1973) 199–209.
[3] D.G. Mashek, K.E. Bornfeldt, R.A. Coleman, J. Berger, D.A. Bernlohr, P. Black, C.C. DiRusso, S.A. Farber, W. Guo, N. Hashimoto, V. Khodiyar, F.A. Kuypers, L.J. Maltais, D.W. Nebert, A. Renieri, J.E. Schaffer, A. Stahl, P.A. Watkins, V. Vasiliou, T.T. Yamamoto, Revised nomenclature for the mammalian long-chain acyl-CoA synthetase gene family, J. Lipid Res. 45 (2004) 1958–1961.
[4] K. Waku, Origins and fates of fatty acyl-CoA esters, Biochim. Biophys. Acta 1124 (1992) 101–111.
[5] N.J. Faergeman, J. Knudsen, Role of long-chain fatty acyl-CoA esters in the regulation of metabolism and in cell signaling, Biochem. J. 323 (1997) 1–12.
[6] M.W. Sleeman, N.P. Donegan, R. Heller-Harrison, W.S. Lane, M.P. Czech, Association of acyl-CoA synthetase-1 with GLUT4-containing vesicles, J. Biol. Chem. 273 (1998) 3132–3135.
[7] N. Pfanner, L. Orci, B.S. Glick, M. Amherdt, S.R. Arden, V. Malhotra, J.E. Rothman, Fatty acyl-coenzyme A is required for budding of transport vesicles from Golgi cisternae, Cell 59 (1989) 95–102.

[8] H.M. Korchak, L.H. Kane, M.W. Rossi, B.E. Corkey, Long chain acyl-coenzyme A and signaling in neutrophils, J. Biol. Chem. 269 (1994) 30281–30287.
[9] T.J. Fitzsimmons, J.A. McRoberts, K.H. Tachiki, S.J. Pandol, Acyl-coenzyme A causes Ca^{2+} release in pancreatic acinar cells, J. Biol. Chem. 272 (1997) 31345–31350.
[10] R. Hertz, J. Magenheim, I. Berman, J. Bar-Tana, Fatty acyl-CoA thioesters are ligands of hepatic nuclear factor 4α, Nature 392 (1998) 512–516.
[11] N. Raman, P.N. Black, C. DiRusso, Characterization of the fatty-acid responsive transcription factor FadR, J. Biol. Chem. 272 (1997) 30645–30650.
[12] P.N. Black, Q. Zhang, J.D. Weimar, C.C. DiRusso, Mutational analysis of a fatty acyl-coenzyme A synthetase signature motif identifies seven amino acid residues that modulate fatty acid substrate specificity, J. Biol. Chem. 272 (1997) 4896–4903.
[13] H.Y. Suzuki, J. Kawarabayasi, T. Kondo, K. Abe, S. Nishikawa, T. Kimura, T. Hashimoto, T. Yamamoto, Structure and regulation of rat long-chain acyl-CoA synthetase, J. Biol. Chem. 265 (1990) 8681–8685.
[14] H. Iijima, T. Fujino, H. Minekura, H. Suzuki, M.J. Kang, T. Yamamoto, Biochemical studies of two rat acyl-CoA synthetases, ACS1 and ACS2, Eur. J. Biochem. 242 (1996) 186–190.
[15] M.J. Kang, T. Fujino, H. Sasano, H. Minekura, N. Yabuki, H. Nagura, H. Iijima, T. Yamamoto, A novel arachidonate-preferring acyl-CoA synthetase is present in steroidogenic cells of the rat adrenal, ovary, and testis, Proc. Natl. Acad. Sci. USA 94 (1997) 2880–2884.
[16] E. Oikawa, H. Iijima, T. Suzuki, H. Sasano, H. Sato, A. Kamataki, H. Nagura, M.J. Kang, T. Fujino, H. Suzuki, T. Yamamoto, A novel acyl-CoA synthetase, ACS5, expressed in intestinal epithelial cells and proliferating preadipocytes, J. Biochem. 124 (1998) 679–685.
[17] T. Fujino, T. Yamamoto, Cloning and functional expression of a novel long-chain acyl-CoA synthetase expressed in brain, J. Biochem. 111 (1992) 197–203.
[18] T. Fujino, M.J. Kang, H. Suzuki, H. Iijima, T. Yamamoto, Molecular characterization and expression of rat acyl-CoA synthetase 3, J. Biol Chem. 271 (1996) 16748–16752.
[19] T. Abe, T. Fujino, R. Fukuyama, S. Minoshima, N. Shimzu, H. Toh, H. Suzuki, T. Yamamoto, Human long-chain acyl-CoA synthetase: structure and chromosomal location, J. Biochem. 111 (1992) 123–128.
[20] K.T. Malhotra, K. Malhotra, B.H. Lubin, F.A. Kuypers, Identification and molecular characterization of acyl-CoA synthetase in human erythrocytes and erythroid precursors, Biochem. J. 344 (1999) 135–143.
[21] J.R. Marszalek, C. Kitidis, A. Dararutana, H.F. Lodish, Acyl-CoA synthetase 2 overexpression enhances fatty acid internalization and neurite outgrowth, J. Biol. Chem. 279 (2004) 23882–23891.
[22] J. Jumpsen, M.T. Clandinin, Brain Development: Relationship to Dietary Lipid and Lipid Metabolism, American Oil Chemists' Society Press, Champaign, IL, 1995.
[23] C.J. Masters, D.I. Crane, On the role of the peroxisome in ontogeny, ageing and degenerative disease, Mech. Ageing Dev. 80 (1995) 69–83.
[24] T.S. Reddy, N.G. Bazan, Long-chain acyl CoA synthetase in microsomes from rat brain gray matter and white matter, Neurochem. Res. 10 (1985) 377–386.
[25] K.K. Vaswani, R.W. Ledeen, Long-chain acyl-coenzyme A synthetase in rat brain myelin, J. Neurosci. Res. 17 (1987) 65–70.
[26] H.J. Kee, J.T. Koh, S.Y. Yang, Z.H. Lee, Y.H. Baik, K.K. Kim, A novel murine long-chain acyl-CoA synthetase expressed in brain participates in neuronal cell proliferation, Biochem. Biophys. Res. Commun. 305 (2003) 925–933.